Numerical Methods in Civil Engineering

Mixed finite element formulation enriched by Adomian method for vibration analysis of horizontally curved beams

A. Moslehi Tabar* H. Najafi Dehkordi**

ARTICLE INFO

Article history:
Received:
November 2016.
Revised:
March 2017.
Accepted:
May 2017.

Keywords:
Mixed finite element; Adomian decomposition method; Out-of-plane vibration; dynamic analysis ; horizontally curved beams.

Abstract:

The vibration analysis of horizontally curved beams is generally led to higher order shape functions using direct finite element method, resulting in more time-consuming computation process. In this paper, the weak-form mixed finite element method was used to reduce the order of shape functions. The shape functions were first considered linear which did not provide adequate accuracy. Accordingly, Adomian decomposition method was employed to enrich the shape functions. As a result, the error percentage reduced significantly. The present method was validated by solving different examples and comparing the results with those reported by other researchers.

1. Introduction

The out-of-plane vibration of curved beams has been analyzed for many years due to its extensive use in many engineering applications. This subject was primarily investigated analytically by Culver 1967[2], Rao 1971[15], Kang and Yoo 1994[9]). However, due to the limitations existing in analytical analyses, the numerical methods such as the finite element method (FEM) drew the attention of researchers.

Several researchers have made efforts to address a specific feature in their finite element formulations. Davis et al. (1972)[3] derived the stiffness and mass matrices from the force-displacement relations and the kinetic energy equations, respectively.The matrices were derived for out-of-plane coupled bending and torsional motions of a curved beam.

The analysis was based upon the exact differential equations of an infinitesimal element in static equilibrium, in which, the effects of transverse shear deformation and transverse rotary inertia were considered. Yoo and Fehrenbach (1981)[19] analyzed the free vibration of horizontally curved beams using finite element method (FEM) and neglecting the effects of shear deformation. By taking into account the effect of warping and rotary inertia due to flexure and torsion, the stiffness and mass matrices of a spatial curved beam element was formulated. Lebeck and Knowlton (1985)[11] used the ring theory to develop the stiffness matrix of a circular beam element considering the coupling between the in-plane and out-of-plane loads and deflections. On the other hand, Howson and Jemah (1999)[6] obtained the out-of-plane frequencies of curved Timoshenko beams using dynamic stiffness matrix, and discussed the effects of shear deflection and rotary inertia. Piovan and Cortinez (2000)[14] addressed the shear deformability due to the bending and warping in their formulations which covered both open and closed cross sections. Yoon et al. (2006)[20] developed an FEM for the free vibration of horizontally thin-walled curved beams. These equations were based on the curved beam theory developed by Kang and Yoo (1994)[9]. The equations of motion governing dynamic behavior of thin-walled curved beams were used with seven degrees of freedom at each

* *Corresponding Author : Assistant Professer, Department of Civil Engineering, Tafresh University ,Tafresh, Iran.*
E-mail: amoslehi@tafreshu.ac.ir
** *Graduate student, Tafresh University,Tafresh, Iran.*

node including the warping degree of freedom. Duan (2008)[4] developed nonlinear vibration of curved beams owing to large deformation.

The effect of eccentricity between the centroid and shear center was addressed in this study. Kim et al. (2009)[10] presented a finite beam element involving the secondary transverse shear deformation, transverse rotary inertia, and torsional rotary inertia. Lee et al. (2002)[12], Chen (2003)[1] and Wu and Chen (2011)[18] generalized the vibration analysis of horizontally curved beams for non-classical supports.

In addition to the use of FEM, some numerical methods such as the differential quadrature method (DQM) and wave propagation method (WPM) have also been employed for the dynamic analysis of curved beams (Kang et al. 1996[7]; Kang et al. 2003[8]).

The previous FEMs developed for the analysis of curved beams were based on the direct method which requires high order shape functions or instead, more element divisions. The main objective of this paper is to reduce the order of shape functions by using mixed finite element formulation. To achieve a specific accuracy, the order of shape functions needed in the mixed finite element is notably lower than those used in the direct finite element (Reddy 2006[16]). In other words, the number of elements may significantly be decreased in case of using the mixed finite element method. In this paper, all the shape functions related to the generalized displacements and forces were first assumed to be linear. However, acceptable natural frequencies were not obtained for curved beams in these conditions. Consequently, the linear displacement shape functions were enriched to cubic ones using Adomian decomposition method (Duan et al. 2012[5]; Mao 2012[13]) while the force shape functions remained linear. Herewith, the results obtained from the present method conformed well with those reported by other researchers.

2. Mathematical Model

Consider a horizontally curved beam as shown in Fig. 1. The radius of curvature and the subtended angle are denoted by R and θ, respectively. The out-of-plane vibration of this beam is governed by the following differential equations [9]:

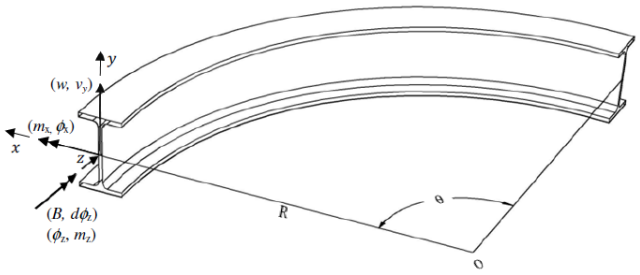

Fig.1: Horizontally curved beam

$$-\frac{\partial v_y}{\partial s}+f_y+\rho A\frac{\partial^2 w}{\partial s^2}=0 \tag{1a}$$

$$\frac{\partial m_x}{\partial s}-\frac{1}{R}\frac{\partial b}{\partial s}+\frac{T_{sv}}{R}-v_y+\rho\left[I_x\frac{\partial^2}{\partial t^2}\left(\frac{\partial w}{\partial s}\right)+\frac{C_w}{R}\frac{\partial^2}{\partial t^2}\left(\frac{\partial \emptyset_z}{\partial s}\right)\right]=0 \tag{1b}$$

$$\frac{m_x}{R}+\frac{\partial^2 b}{\partial s^2}-\frac{\partial T_{sv}}{\partial s}+t_z+\rho J_0\frac{\partial^2 \emptyset_z}{\partial t^2}-\rho\left[C_w\frac{\partial^2}{\partial t^2}\left(\frac{\partial \emptyset_z}{\partial s}\right)+\frac{C_w}{R}\frac{\partial^2}{\partial t^2}\left(\frac{\partial w}{\partial s}\right)\right]=0 \tag{1c}$$

where v_y, m_x, T_{sv}, b denote shear force, bending moment about x axis, St. Venant torsion, and bimoment, respectively. The other parameters are defined as: cross sectional area (A); moment of inertia about x and y-axes (I_x and I_y); warping moment of inertia (C_w); St. Venant constant (J); modulus of elasticity (E); shear modulus of elasticity (G); mass density (ρ); polar moment of inertia (J_0).

These internal actions are expressed in terms of the generalized displacements as:

$$\frac{m_x}{EI_x}=-\frac{\partial^2 w}{\partial s^2}+\frac{\emptyset_z}{R} \tag{2a}$$

$$\frac{T_{sv}}{GJ}=\frac{\partial \emptyset_z}{\partial s}+\frac{1}{R}\frac{\partial w}{\partial s} \tag{2b}$$

$$\frac{b}{EC_w}=\frac{\partial^2 \emptyset_z}{\partial s^2}+\frac{1}{R}\frac{\partial^2 w}{\partial s^2} \tag{2c}$$

2.1 Mixed finite element formulation

The combination of the differential Eqs. 1 and 2 results in an eighth-order differential equation which generally includes a hard solution. To reduce the order of unknown functions, a weak-form finite element formulation was used in this paper. To this end, the variables w, ϕ, m_x, $b$are assumed to be independent. Consequently, the weak-form finite element is formulated as below:

$$\int_0^{s_0}\delta w\left(\frac{\partial^2 m_x}{\partial s^2}-\frac{1}{R}\frac{\partial^2 b}{\partial s^2}+\frac{GJ}{R}\frac{\partial^2 \emptyset_z}{\partial s^2}+\frac{GJ}{R^2}\frac{\partial^2 w}{\partial s^2}+\rho\left[I_x\frac{\partial^2}{\partial t^2}\left(\frac{\partial^2 w}{\partial s^2}\right)+\frac{C_w}{R}\frac{\partial^2}{\partial t^2}\left(\frac{\partial^2 \emptyset_z}{\partial s^2}\right)\right]-f_y+\rho A\frac{\partial^2 w}{\partial t^2}\right)ds=0 \tag{3a}$$

$$\int_0^{s_0} \delta\emptyset_z \left(\frac{m_x}{R} + \frac{\partial^2 b}{\partial s^2} - \frac{GJ}{R}\frac{\partial^2 \emptyset_z}{\partial s^2} - \frac{GJ}{R^2}\frac{\partial^2 w}{\partial s^2} + t_z + \rho J \frac{\partial^2 \emptyset_z}{\partial t^2} - \frac{\rho C_w}{E C_w}\frac{\partial^2 b}{\partial t^2} \right) ds = 0 \quad (3b)$$

$$\int_0^{s_0} \delta m_x \left(\frac{m_x}{EI_x} + \frac{\partial^2 w}{\partial s^2} - \frac{\emptyset_z}{R} \right) ds = 0 \quad (3c)$$

$$\int_0^{s_0} \delta b \left(\frac{b}{EC_w} - \frac{\partial^2 \emptyset_z}{\partial s^2} - \frac{1}{R}\frac{\partial^2 w}{\partial s^2} \right) ds = 0 \quad (3d)$$

The generic functions w, ϕ, m_x, b, are interpolated based on the corresponding nodal values, i.e. W, Φ, M_x, B:

$$w(s) = N_w(s)W \; ; \; \emptyset_z(s) = N_\emptyset(s)\Phi_z \; ; \; m_x(s) = N_m(s)M_x \; ; \; b(s) = N_b(s)B \quad (4)$$

where N_w, N_f, N_m and N_b are the shape functions generalizing the nodal displacement, torsion, moment and bimoment, respectively.

Replacing Eq. 4 into Eqs. 3, the following relations yield:

$$\frac{GJ}{R^2}\int_0^{s_0} N_{ws}^T . N_{ws} ds \; W - \frac{GJ}{R}\int_0^{s_0} N_{ws}^T . N_{\phi s} ds \, \Phi_z + \int_0^{s_0} N_{ws}^T . N_{ms} ds \, M_x = V_y + \int_0^{s_0} N_w^T f_y ds \quad (5a)$$

$$-\frac{GJ}{R}\int_0^{s_0} N_{\phi s}^T . N_{ws} ds \; W + GJ \int_0^{s_0} N_{\phi s}^T . N_{\phi s} ds \, \Phi_z - \frac{1}{R}\int_0^{s_0} N_\phi^T . N_m \, ds \, M_x + \int_0^{s_0} N_{\phi s}^T . N_{bs} ds \; B = m_z + \int_0^{s_0} N_\phi^T t_z ds \quad (5b)$$

$$\int_0^{s_0} N_{ms}^T . N_{ws} ds \; W - \frac{1}{R}\int_0^{s_0} N_m^T . N_\phi \, ds \, \Phi_z - \frac{1}{EI_x}\int_0^{s_0} N_m^T . N_m \, ds \, M_x = \Phi_x \quad (5c)$$

$$\int_0^{s_0} N_{bs}^T . N_{\phi s} ds \, \Phi_z + \frac{1}{EC_w}\int_0^{s_0} N_b^T . N_b \; ds \, B = d\Phi_z \quad (5d)$$

The Eqs. (5a) to (5d) may be rewritten in the matrix form as follows:

$$\begin{bmatrix} \mu_{11} \mu_{12} \mu_{13} \mu_{14} \\ \mu_{21} \mu_{22} \mu_{23} \mu_{24} \\ \mu_{31} \mu_{32} \mu_{33} \mu_{34} \\ \mu_{41} \mu_{42} \mu_{43} \mu_{44} \end{bmatrix} \begin{Bmatrix} \ddot{W} \\ \ddot{\Phi}_z \\ \ddot{M}_x \\ \ddot{B} \end{Bmatrix} + \begin{bmatrix} \chi_{11} \chi_{12} \chi_{13} \chi_{14} \\ \chi_{21} \chi_{22} \chi_{23} \chi_{24} \\ \chi_{31} \chi_{32} \chi_{33} \chi_{34} \\ \chi_{41} \chi_{42} \chi_{43} \chi_{44} \end{bmatrix} \begin{Bmatrix} W \\ \Phi_z \\ M_x \\ B \end{Bmatrix} = \begin{Bmatrix} V_y + V_{yf} \\ M_z + M_{zt} \\ \Phi_x \\ d\Phi_z \end{Bmatrix} \quad (6)$$

in which

$$V_{yf} = \int_0^{s_0} N_w^T f_y ds; \quad M_{zt} = \int_0^{s_0} N_\emptyset^T t_z ds \quad (7)$$

The coefficient matrix χ denotes the mixed stiffness-flexibility matrix with the elements χ_{ij}defined as below:

$$\chi_{11} = \frac{GJ}{R^2}\int_0^{s_0} N_{ws}^T . N_{ws} ds \; ; \quad \chi_{12} = -\frac{GJ}{R}\int_0^{s_0} N_{ws}^T . N_{\phi s} ds \; ; \quad \chi_{13} = \int_0^{s_0} N_{ws}^T . N_{ms} ds \quad \chi_{14} = 0$$

$$\chi_{21} = -\frac{GJ}{R}\int_0^{s_0} N_{\phi s}^T . N_{ws} ds \; ; \quad \chi_{22} = GJ \int_0^{s_0} N_{\phi s}^T . N_{\phi s} ds; \quad \chi_{23} = -\frac{1}{R}\int_0^{s_0} N_\phi^T . N_m \, ds$$

$$\chi_{24} = \int_0^{s_0} N_{\phi s}^T . N_{bs} ds \quad (8)$$

$$\chi_{31} = \int_0^{s_0} N_{ms}^T . N_{ws} ds \; ; \quad \chi_{32} = -\frac{1}{R}\int_0^{s_0} N_m^T . N_\phi \; ds; \quad \chi_{33} = -\frac{1}{EI_x}\int_0^{s_0} N_m^T . N_m \, ds \quad \chi_{34} = 0$$

$$\chi_{41} = 0; \quad \chi_{42} = \int_0^{s_0} N_{bs}^T . N_{\phi s} ds; \quad \chi_{43} = 0; \quad \chi_{44} = \frac{1}{EC_w}\int_0^{s_0} N_b^T . N_b \; ds$$

The matrix elements μ_{ij} are derived as follows:

$$\mu_{11} = \rho A \int_0^{s_0} N_w^T . N_w \, ds; \mu_{12} = \mu_{13} = \mu_{14} = 0$$
$$\mu_{21} = 0; \ \mu_{22} = \rho J_0 \int_0^{s_0} N_\phi^T . N_\phi \, ds; \mu_{23} = \mu_{24} = 0 \quad (9)$$
$$\mu_{31} = \mu_{32} = \mu_{33} = \mu_{34} = 0$$
$$\mu_{41} = \mu_{42} = \mu_{43} = \mu_{44} = 0$$

This is in the form of lumped mass matrix if the shape functions are assumed to be linear.

2.2 Enrichment of shape functions using Adomian decomposition method (ADM)

The above-mentioned finite element may become more accurate using higher order shape functions. In this paper, the Adomian decomposition method (Duan et al. 2012[5]; Mao 2012[13]) was used to enrich shape functions. For this purpose, Eq. 1(c) is rewritten as below:

$$\frac{\partial^2 \emptyset_z}{\partial s^2} = \frac{1}{R.GJ} m_x + \frac{1}{GJ}\frac{\partial^2 b}{\partial s^2} - \frac{1}{R}\frac{\partial^2 w}{\partial s^2} \quad (10)$$

The following equation is obtained by double integration of Eq. 10,

$$\emptyset_z(s) = \emptyset_{z0} + \emptyset'_{z0} s + \int_0^s \int_0^s \left[\frac{1}{R.GJ} m_x + \frac{1}{GJ}\frac{\partial^2 b}{\partial s^2} - \frac{1}{R}\frac{\partial^2 w}{\partial s^2}\right] ds.ds \quad (11)$$

In Adomian method, the solution $\emptyset_z$ is commonly taken as

$$\emptyset_z(s) = \sum_{n=0}^{\infty} \emptyset_{zn} \quad (12)$$

and the integrand on the right side as

$$\frac{1}{R.GJ} m_x + \frac{1}{GJ}\frac{\partial^2 b}{\partial s^2} - \frac{1}{R}\frac{\partial^2 w}{\partial s^2} = \sum_{n=0}^{\infty} A_n(\emptyset_{z0}, \emptyset_{z1}, \dots., \emptyset_{zn}) \quad (13)$$

Substituting Eqs. 12 and 13 into Eq. 11, yields

$$\sum_{n=0}^{\infty} \emptyset_{zn} = \emptyset_{z0} + \emptyset'_{z0} s + \sum_{n=0}^{\infty} \int_0^s \int_0^s A_n(\emptyset_{z0}, \emptyset_{z1}, \dots., \emptyset_{zn}) \, ds.ds \quad (14)$$

in which

$$\emptyset_{z0} := \emptyset_{z0} + \emptyset'_{z0} s \quad (15a)$$
$$\emptyset_{zn+1} := \int_0^s \int_0^s A_n(\emptyset_{z0}, \emptyset_{z1}, \dots., \emptyset_{zn}) \, ds.ds \quad (15b)$$

$n = 0,1,2, \dots..$

The solution $\emptyset_z$ may be estimated more accurately by employing more iterations. For the first-order estimation, *b* and *w* functions are considered linear and their second derivatives are then zero. Thus, using the boundary conditions as

$$\emptyset_{z0} = \emptyset_z(0) = \Phi_{z1}$$

$$\emptyset'_{z0} = \left.\frac{d\emptyset_z}{ds}\right|_{s=0}$$

the following relation yields for $\emptyset_z$ after one iteration based on ADM:

$$\emptyset_z(s) = N_\phi \Phi_z + \frac{R}{GJ}\frac{s_0^2}{R^2} N_M M_x \quad (16)$$

where

$$N_\phi(s) = \left[1 - \frac{s}{s_0}\frac{s}{s_0}\right] \quad (17a)$$
$$N_M(s) = \left[\frac{1}{3}\left(\frac{s}{s_0}\right) - \frac{1}{2}\left(\frac{s}{s_0}\right)^2 + \frac{1}{6}\left(\frac{s}{s_0}\right)^3 \frac{1}{6}\left(\frac{s}{s_0}\right) - \frac{1}{6}\left(\frac{s}{s_0}\right)^3\right] \quad (17b)$$

In essence, by using the ADM, the generalized displacement $\emptyset_z$ is coupled with the end moments using cubic interpolation functions.

A similar process is performed on Eq. 2(a) to enhance *w* function, as follows:

$$\frac{\partial^2 w}{\partial s^2} = -\frac{m_x}{EI_x} + \frac{\emptyset_z}{R} \quad (18)$$

By performing double integration of Eq. 18:

$$w(s) = w_0 + \acute{w_0} s + \int_0^s \int_0^s \left[-\frac{1}{EI} m_x + \frac{1}{R}\emptyset_z\right] ds.ds \quad (19)$$

Using the boundary conditions as

$$w_0 = w(0) = W_1$$

$$\acute{w_0} = \left.\frac{dw}{ds}\right|_{s=0}$$

the following relation yields for *w*

$$w(s) = N_w W + \frac{R^2}{EI}\frac{s_0^2}{R^2} N_M M_x - \frac{s_0^2}{R} N_\Phi \Phi_z \quad (20)$$

where

$$N_W(s) = \left[1 - \frac{s}{s_0}\frac{s}{s_0}\right] \quad (21a)$$

$$N_{\Phi}(s)=\left[\frac{1}{3}\left(\frac{s}{s_0}\right)-\frac{1}{2}\left(\frac{s}{s_0}\right)^2+\frac{1}{6}\left(\frac{s}{s_0}\right)^3\frac{1}{6}\left(\frac{s}{s_0}\right)-\frac{1}{6}\left(\frac{s}{s_0}\right)^3\right] \quad (21b)$$

According to Eq. 20, the generalized displacement w relates to the end moments, M_x, and end twists, $\emptyset_z$. The functions developed as Eqs. 16 and 20 may become more accurate using successive iteration of ADM.

By replacing the enriched shape functions into Eq. 3, the elements of the stiffness and mass matricesare changed as follows:

$$\begin{aligned}\chi_{23}&=-\frac{1}{R}\int_0^{s_0}N_{\phi}^T.N_m\,ds-\frac{1}{R}\int_0^{s_0}N_{\phi}^T.N_M\,ds\\ \chi_{32}&=-\frac{1}{R}\int_0^{s_0}N_m^T.N_{\phi}\,ds-\frac{1}{R}\int_0^{s_0}N_m^T.N_{\Phi}\,ds\\ \chi_{33}&=-\frac{1}{EI_x}\int_0^{s_0}N_m^T.N_m\,ds-\frac{1}{GJ}\int_0^{s_0}N_m^T.N_M\,ds\end{aligned} \quad (22)$$

and;

$$\begin{aligned}\mu_{12}&=\mu_{21}=\rho A\int_0^{s_0}N_w^T.N_{\Phi}\,ds\\ \mu_{13}&=\mu_{31}=\frac{R\rho A}{EI_x}\int_0^{s_0}N_w^T.N_{\mathrm{M}}\,ds\end{aligned} \quad (23)$$

The other elements remain unchanged.

It is worthy to note that by using enriched shape functions, the mass matrix is converted to the consistent matrix as compared with the lumped mass matrix derived by Eq. 9. Furthermore, the shape functions related to the moment and bi-moment are still assumed linear in this paper.

3. Numerical Verifications

To verify the present formulation and the effect of the enriched shape functions, two examples are investigated in the following. For the simple supports studied in these examples, the degrees of freedom related to the displacement and twist at the supports are restrained. In order to apply boundary conditions, the rows and columns of the stiffness and mass matrices, corresponding to the restrained degrees of freedom, are eliminated.

3.1 Example 1

A curved beam with length of L=10.16m is assumed as shown in Fig. 2. The simple support conditions are considered for both ends. By taking the beam length to be constant, the subtended angle of the curve is changed from zero (straight beam) to 90 degree (a quadrant). The geometrical and mechanical properties of the beam are given in Table 1.

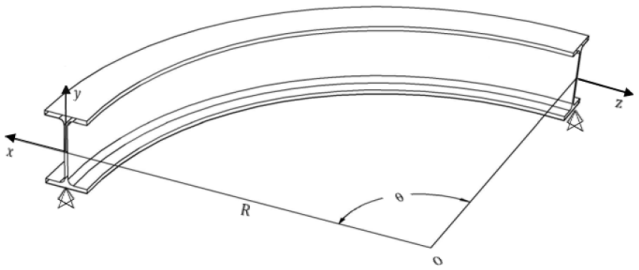

Fig. 2: A simply supported curved beam

Table 1: Geometrical and mechanical properties of curved beam

Cross sectional area (*A*)	9.292×10^{-3} m^2
Moment of inertia about *x*-axis (I_x)	1.134×10^{-4} m^4
Moment of inertia about *y*-axis (I_y)	3.886×10^{-5} m^4
Warping moment of inertia (C_w)	5.559×10^{-7} m^6
St. Venant constant (*J*)	5.386×10^{-7} m^4
Modulus of elasticity (*E*)	200 GPa
Shear modulus of elasticity (*G*)	77.2 GPa
Mass density (ρ)	7855 kg/m^3

Four natural frequencies obtained from the present formulation are given in Table 2. As observed in the table, the fourth frequency cannot be extracted for more straight beams because, the fourth frequency relates to twist and the beams with less subtended angle have insignificant twisting mass.

Table 2: Two fundamental natural frequencies for Example 1

Angle (degree)	ω_1 (rad/s)	ω_2 (rad/s)	ω_3 (rad/s)	ω_4 (rad/s)
0	53.78	213.98	481.87	-
10	31.96	139.74	286.01	-
20	19.93	114.66	266.16	-
30	13.98	95.54	245.35	-
40	10.55	80.85	225.71	-
50	8.34	69.42	207.54	-
60	6.77	60.36	185.64	2052.0
70	5.59	53.11	171.18	2160.3
80	4.64	47.26	158.24	2365.4
90	3.85	42.41	145.55	2605.8

The accuracy of the first natural frequencies are compared with previous results (Yoon et al. 2006[20]) in Table 3.It should be noted that the present results are based on the models that are divided into just two elements. As observed in the table, the present mixed formulation with linear shape functions has significant error even in case of the straight beam (zero subtended angle). In case of the quadrant curve (90 degree subtended angle), the calculation error is about 60 percent and, of course, not acceptable. However, the calculation errors reduced considerably by using enriched shape functions resulting from ADM. The errors involved in this case are less than one percent. The fundamental frequency is revealed versus different subtended angles in Fig.3. The figure confirms that the results with assumption of the enriched shape functions correlate well with the analytical and previous solutions. According to Eqs. (16) and (20), the shape functions of ϕ and *w* were upgraded from linear to cubic functions using one iteration in the Adomian method while the other shape functions were kept linear.

Table 3: Comparison of the first natural frequencies for Example 1

Angle (degree)	Analytical	Yoon et al. (2006)		Present (Linear)		Present (enhanced)	
		ω(rad/s)	Error(%)	ω(rad/s)	Error(%)	ω(rad/s)	Error(%)
0	53.80	53.80	0.00	64.84	20.52	53.78	0.04
10	31.86	31.87	0.03	40.62	27.50	31.96	0.31
20	19.96	19.96	0.00	26.56	33.07	19.93	0.15
30	13.99	13.99	0.00	19.09	36.45	13.98	0.07
40	10.54	10.54	0.00	14.66	39.09	10.55	0.09
50	8.29	8.29	0.00	11.77	41.98	8.34	0.60
60	6.71	6.70	0.15	9.73	45.01	6.77	0.89
70	5.53	5.51	0.36	8.21	48.46	5.59	1.08
80	4.60	4.57	0.65	7.02	52.61	4.64	0.87
90	3.85	3.80	1.30	6.04	56.88	3.85	0.00

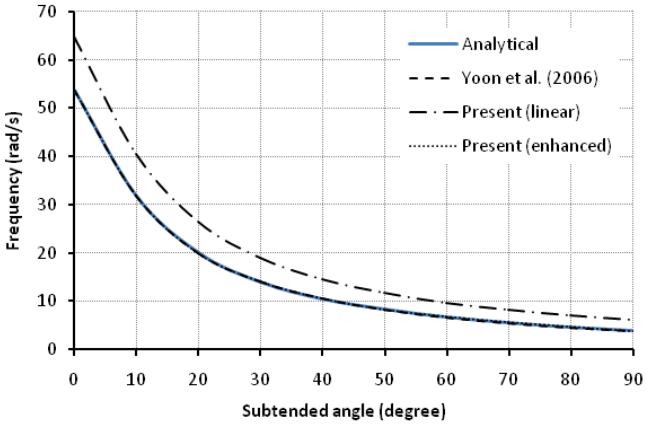

Fig. 3: Frequency-subtended angle curves for Example 1

By enhancing the displacement shape functions, not only do the coefficient matrices become more accurate, but the relations between different variables is also enriched.

3.2 Example 2

In the second example, the length of the curved beam is assumed to be 5.12 m. while the other geometrical and mechanical properties are the same as those noted in Table 1 with the exception of J which is taken as 1.471×10^{-5} m^4. This implies that the curved beam assumed in this example possesses more torsional rigidity. The subtended angle of the curve is changed from 10 degree to 90 degree while the beam length is fixed.

The natural frequencies estimated according to this study are compared with those obtained by Yoo and Fehrenbach (1981)[19] and Yoon et al. (2006)[20] as given in Table 4. The linear shape functions are not accurate again with some errors exceeding 30 percent in this case. Whereas, by using enriched shape functions, the errors decreased notably down to the range of 0.1 to 4.1 percent. The fundamental frequency is depicted versus different subtended angles in Fig. 4. An obviously good agreement is inferred between the results with the assumption of enriched shape functions and the previous solutions.

4. Conclusions

A mixed finite element formulation was used for dynamic analysis of horizontally curved beams. The direct finite element solution of a horizontally curved beam is generally led to higher order shape functions, resulting in more time-consuming computation process. In this paper, the weak-form mixed finite element method was used to reduce the order of shape functions. In this case, the shape functions were initially considered linear which did not provide adequate accuracy. Accordingly, the shape functions were enriched using ADM. As a result, the error percentage was dramatically reduced. In essence, by enhancing the displacement shape functions, the coefficient matrices become more accurate on one hand, and the relations between different variables is enriched on the other hand. According to the examples solved in the paper, the results obtained from the proposed method were comparable with those reported by other researchers.

Acknowledgments

This research forms parts of a project funded by Iranian Railway Administration of Tracks and Technical Structures under Contract No. 31SAD/4986. Their support is gratefully acknowledged by the authors. Any opinions presented in this paper, however, are the authors' alone, and not necessarily the sponsor's.

Table 4: Comparison of the first natural frequencies for Example 2

Angle (degree)	Yoo and Fehrenbach (1981)	Yoon et al. (2006)		Present (Linear)		Present (enhanced)	
	ω (rad/s)	ω(rad/s)	Error(%)	ω(rad/s)	Error(%)	ω (rad/s)	Error(%)
10	204.7	201.3	1.7	247.2	20.8	204.9	0.1
20	190.2	183.2	3.7	228.1	19.9	188.1	1.1
30	165.8	160.9	3.0	204.1	23.1	166.7	0.5
40	141.7	139.5	1.6	179.7	26.8	144.9	2.3
50	121.3	120.1	1.0	156.9	29.3	124.6	2.7
60	103.9	103.0	0.9	136.3	31.2	106.4	2.4
70	89.3	88.3	1.1	117.8	31.9	90.1	0.9
80	76.8	75.4	1.8	100.9	31.4	75.3	2.0
90	64.0	64.1	0.2	85.2	33.1	61.4	4.1

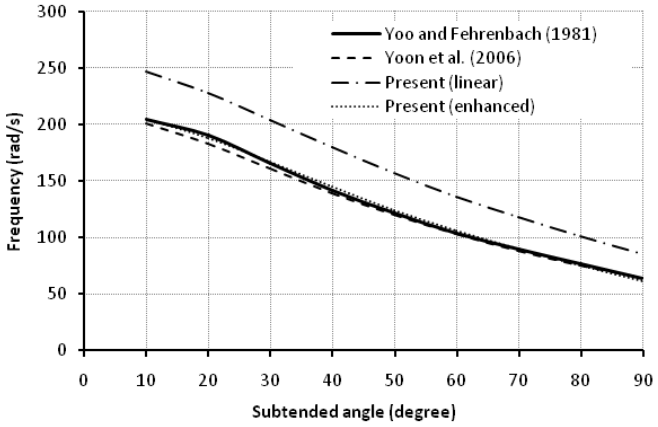

Fig. 4: Frequency-subtended angle curves for Example 2

References

[1]Chen, D. W., "The exact solutions for natural frequencies and mode shapes of non-uniform beams carrying multiple various concentrated elements", Struct. Eng. Mech., vol. 16, 2003, p. 153-176.

[2]Culver, C. G., "Natural frequencies of horizontally curved beams", J. Struct. Eng., vol. 93, 1967, p. 189-203.

[3]Davis, R., Henshell, R. D., and Warburton, G. B., "Curved beam finite elements for coupled bending and torsional vibration", Earthquake Eng. Struct. Dynam, vol. 1, 1972, p. 165-175.

[4]Duan, H., "Nonlinear free vibration analysis of asymmetric thin-walled circularly curved beams with open cross section", Thin-Walled Struct., vol. 46, 2008, p. 1107-1112.

[5]Duan, J. S., Rach, R., Baleanu, D., and Wazwaz, A. M., "A review of the Adomian decomposition method and its applications to fractional differential equations" Commun. Frac. Calc, vol. 3, 2012, p. 73-99.

[6]Howson, W. P., and Jemah, A. K., "Exact out-of-plane natural frequencies of curved Timoshenko beams", J.Eng. Mech., vol. 123, 1999, p. 19-25.

[7]Kang, K., Bert, C. W., and Striz, A. G., "Vibration Analysis of Horizontally Curved Beams with Warping Using DQM", J. Struct. Eng., vol. 122, 1996, p. 657 – 662.

[8]Kang, B., Riedel, C. H., and Tan, C. A., "Free vibration analysis of planar curved beams by wave propagation", J. Sound Vib., vol. 260, 2003, p. 19-44.

[9]Kang, Y. J., and Yoo, C. H., "Thin-walled curved beams, I: formulation of nonlinear equations", J.Eng. Mech., vol. 120, 1994, p. 2072-2101.

[10]Kim, B. Y., Kim, C. B., Song, S. G., Beom, H. G., and Cho, C., "A finite thin circular beam element for out-of-plane vibration analysis of curved beams", J. Mech. Sci. Technol., vol. 23, 2009, p. 1396-1405.

[11]Lebeck, A. O., and Knowlton, J. S., "A finite element for the three-dimensional deformation of a circular ring", Int. J. Numer. Meth. Eng., vol. 21, 1985, p. 421-435.

[12]Lee, B. K., Oh, S. J., and Park, K. K., "Free vibrations of shear deformable circular curved beams resting on elastic foundation", Int. J. Struct. Stab. Dyn., vol. 2, 2002, p. 77-97.

[13]Mao, Q., "Free vibration analysis of elastically connected multiple-beams by using the Adomian modified decomposition method", J. Sound Vib., vol. 331, 2012, p. 2532-2542.

[14]Piovan, M. T., and Cortinez, V. H., "Out-of-plane vibrations of shear deformable continuous horizontally curved thin-walled beams", J. Sound Vib., vol. 237, 2000, p. 101-118.

[15]Rao, S. S., "Effects of transverse shear and rotatory inertia on the coupled twist-bending vibrations of circular rings", J. Sound Vib., vol. 16, 1971, p. 551–566.

[16]Reddy, J. N., An introduction to the finite element method, 3rd Ed., McGraw Hill, New York, 2006.

[17]Shore, S., and Chaudhuri, S., "Free vibration of horizontally curved beams", J. Struct. Eng., vol. 98, 1972, p. 793 – 796.

[18]Wu, J. S., and Chen, Y. C., "Out-of-plane free vibration analysis of a horizontally circular curved beam carrying arbitrary sets of concentrated elements", J. Struct. Eng., vol. 137, 2011, p. 220-241.

[19]Yoo, C. H., and Fehrenbach, J. P., "Natural frequencies of curved girders", J. Eng. Mech., vol. 107, 1981, p. 339–354.

[20]Yoon, K. Y., Park, N. H., Choi, Y. J., and Kang, Y. J., "Natural frequencies of thin-walled curved beams", Finite Elem. Anal. Des, vol. 42, 2006, p. 1176-1186.